Title

Reduction of myeloid-derived suppressor cells reinforces the anti-solid tumor effect of recipient leukocyte infusion in murine neuroblastoma-bearing allogeneic bone marrow chimeras.

Authors

Isabelle Dierckx de Casterlé[1], Sabine Fevery[1], Omer Rutgeerts[1], Fariba Poosti[2], Sofie Struyf[2], Caroline Lenaerts[1], Mark Waer[1], An D. Billiau[1] and Ben Sprangers[1,3*]

Author affiliations

[1]Department of Microbiology and Immunology, Laboratory of Experimental Transplantation, Katholieke Universiteit (KU) Leuven, Herestraat 49, 3000 Leuven, Belgium

[2]Department of Microbiology and Immunology, Laboratory of Molecular Immunology, KU Leuven, Herestraat 49, 3000 Leuven, Belgium

[3]Department of Nephrology, University Hospitals Leuven, Herestraat 49, 3000 Leuven, Belgium

***** Corresponding Author:

Ben Sprangers

Herestraat 49, box 811, 3000 Leuven, Belgium

ben.sprangers@uzleuven.be

Tel: +32(0)16344580

Abstract

Allogeneic hematopoietic stem cell transplantation is an emerging treatment option for solid tumors because of its capacity to elicit immune graft-*versus*-tumor effects. However, these are often limited and associated with GvHD. Adoptive recipient leukocyte infusion (RLI) was shown to enhance anti-tumor responses of allogeneic bone marrow transplantation in murine neuroblastoma (Neuro2A)-bearing chimeras. In contrast to the clinically used donor leukocyte infusion, the RLI anti-tumor effect –elicited by host-*versus*-graft lymphohematopoietic reactivity– does not cause GvHD; however the tumor growth-inhibitory effect is incomplete because overall survival is not prolonged. Here, we studied the anti-solid tumor mechanisms of RLI with the objective to improve its efficacy. Host-*versus*-graft reactivity following RLI was associated with a systemic cytokine storm, lymph node DC activation and systemic expansion of host-derived IFN-γ-expressing $CD4^+$T cells and IFN-γ-and granzyme B-expressing $CD8^+$T cells, which acquired killing activity against Neuro2A and third-party tumor cells. The tumor showed up-regulation of MHC class I and a transient accumulation of IFN-γ-and granzyme B-expressing $CD8^+$T cells: the intra-tumor decline in cytotoxic $CD8^+$T cells coincided with a systemic –and to a lesser extent intra-tumoral– expansion of MDSC. *In vivo* MDSC depletion with 5-FU significantly improved the local tumor growth-inhibitory effect of RLI as well as overall survival. In conclusion, the RLI-induced alloreactivity gives rise to a host-derived cytotoxic T cell anti-neuroblastoma response, but also drives an expansion of host-type MDSC that counteracts the anti-tumor effect. This finding identifies MDSC as a novel target to increase the effectiveness of RLI, and possibly other cancer immunotherapies.

Keywords

Neuroblastoma - Allogeneic hematopoietic stem cell transplantation - Recipient leukocyte infusion - Cytotoxic T lymphocytes - Myeloid-derived suppressor cells

Précis

This work identifies MDSC as a key intervention target to improve the efficacy of RLI, and points to the need for combination therapies to counteract immune regulatory pathways that may limit the effectiveness of cancer immunotherapies.

Abbreviations

AlloBMT	Allogeneic bone marrow transplantation
AlloHSCT	Allogeneic hematopoietic stem cell transplantation
APC	Allophycocyanin
CBA	Cytometric bead array

CCL2	Chemokine (C-C motif) ligand 2
DLI	Donor leukocyte infusion
FasL	Fas ligand
GvHD	Graft-*versus*-host disease
GvT	Graft-*versus*-tumor
iNKT	Invariant natural killer T cells
M-/G-MDSC	Monocytic/Granulocytic myeloid-derived suppressor cells
MHC-I	MHC class I
MHC-II	MHC class II
NO	Nitric oxide
NOD/SCID	Nonobese diabetic/severe combined immunodeficiency
RLI	Recipient leukocyte infusion
Th1	T helper 1 cells
Treg	T regulatory cells

Introduction

Allogeneic hematopoietic stem cell transplantation (alloHSCT) has been the cornerstone in the treatment of hematological malignancies for decades [1], and is now also emerging as a treatment option for solid tumors, such as renal cell carcinoma, breast cancer [2], and neuroblastoma (clinicaltrials.gov) [3,4]. The therapeutic effect of alloHSCT has been attributed to donor T cells attacking the tumor (graft-*versus*-tumor (GvT) effect). However, donor T cells may also target healthy recipient tissues, resulting in GvHD, causing important morbidity and mortality. Removal of T cells from the donor graft obviates GvHD but results in higher relapse rates [5]. This has led to the use of post-transplant donor leukocyte infusion (DLI) to re-enforce anti-tumor responses. DLI can reinduce remission in patients with post-transplant relapse: a strong lymphohematopoietic donor-anti-host response occurs with rapid conversion of mixed towards full donor chimerism, which is accompanied by effective GvT effects. However, the risk for GvHD, albeit lower than immediately after transplantation, is still significant [6] which stimulates research into safer alternatives to enhance anti-tumor effects after alloHSCT.

Adoptive cell therapy with non-tolerant recipient-type –rather than donor-type– leukocytes (recipient leukocyte infusion, RLI) has recently been explored experimentally, inspired by the observation that some advanced hematological cancer patients who showed spontaneous loss of the donor graft still experienced remission [7]. Studies in murine leukemia models performed by our group and others have shown that RLI can indeed mount anti-leukemia effects when given after allogeneic BMT (alloBMT). RLI into tolerant mixed BM chimeras provokes a lymphohematopoietic host-*versus*-graft reaction resulting in full rejection of the donor graft while producing anti-tumor responses and –importantly– leaving host tissues intact. The observed anti-leukemia mechanisms are thought to be elicited by the alloreactivity and presumed to involve activated host APC that cross-present allogeneic and tumor Ags and in turn activate host $CD4^+$ and $CD8^+$ T cells as well as invariant natural killer T (iNKT) cells and NK cells, but also direct reactivity of RLI-derived non-tolerant IFN-γ-producing $CD8^+$ T cells against the host tumor [8–11].

The potential of RLI to reinforce post-transplant anti-leukemia reactivity without provoking GvHD and the growing interest in alloHSCT for therapy-resistant solid tumors, led us to explore RLI in a solid tumor mouse model, specifically neuroblastoma [12]. Neuroblastoma is the most common extra-cranial solid tumor in childhood. The majority of patients is diagnosed with high-risk disease and faced with poor prognosis despite intensive therapy. Although the currently available treatment has improved the patients outcome over the last few years, high treatment-related toxicity and relapse rates still cause high mortality rates, urgently calling for further research into novel strategies [13,14]. Available clinical data show that alloHSCT is feasible to exploit graft-*versus*-neuroblastoma responses and improve the outcome, but disease recurrence remains the major cause of treatment failure [3,4].

We found in allogeneic BM transplanted mice carrying neuroblastoma that RLI delays local growth and metastasis of neuroblastoma [12], providing first evidence that RLI may effectively target a solid tumor. However, although local tumor growth is significantly reduced by RLI, the tumor-inhibitory effect is incomplete since overall survival is not prolonged. In the present study we aimed to gain a detailed insight into the dynamics and mechanisms of the anti-neuroblastoma response of RLI, with the objective to define a strategy to optimize the efficacy.

Materials and methods

Mice

Female A/J ($H2K^k$, 12-weeks-old) recipient mice and C57Bl/6 ($H2K^b$, 8-weeks-old) donor mice were obtained from Envigo (Venray, The Netherlands; Camebridgeshire, UK) and Janvier Labs (Saint Berthevin, France). Transplanted mice received water supplemented with enrofloxacine (Baytril® 10% 2ml/l) as prophylaxis post-irradiation.

Tumor cell lines

The Neuro2A tumor cell line (ATCC, Rockville, MD, USA) is a cell line derived from a neuroblastoma tumor that spontaneously arose in A/J mice [15]. Experimental tumors are induced by s.c. inoculation of $1x10^6$ Neuro2A cells into the left flank.

The P815 cell line (ATCC) is a mastocytoma-derived tumor cell line used as target cell line for *in vitro* cytotoxicity assays.

Allogeneic BMT

Recipient A/J mice received 9 Gray total body irradiation prior to transplantation (day -1). On day 0 reconstitution with allogeneic hematopoietic stem cells was performed as described previously [16]. BM cells were harvested from the tibias and femurs of donor C57Bl/6 mice. T cells were depleted from the donor marrow using cytotoxic complement-fixing anti-Thy1.2 and low-toxic rabbit complement (Serotec, Oxford, UK). Finally, $5x10^6$ T cell-depleted allogeneic BM cells were injected i.v. into a tail vein of A/J recipient mice.

Recipient leukocyte infusion and MDSC depletion

Spleens were harvested from naive A/J mice and single cell suspensions were prepared using a GentleMACS Dissociator (Myltenyi Biotec, Leiden, The Netherlands). Cells were filtered and rinsed twice with RPMI1640. $50x10^6$ splenocytes/250µl RPMI1640 were injected i.v. into a tail vein of A/J chimeras at day 21 post-alloBMT.

For *in vivo* MDSC depletion, mice were injected i.p. with 5-FU at 50mg/kg body weight on day 30 post-alloBMT.

In vitro CD8 T lymphocyte cytotoxicity assay

To evaluate *in vitro* cytotoxicity of effector $CD8^+$ T cells from chimeric mice, standard ^{51}Cr-release assays were performed. In brief, $CD8^+$ T cells were isolated using MACS, according to the manufactures' instructions. Target tumor cells were labeled with ^{51}Cr (MP Biomedicals, Irvine, CA; 100 µCi/test), followed

by a 4 hour-incubation at 37°C with MACS-purified $CD8^+$ T cells. After incubation, supernatant was collected and ^{51}Cr release was measured using a Topcount gamma counter (Packard Instrument Company, Meriden, USA).

Trypan blue exclusion assay and proliferation assay

To study the direct tumor killing effect of IFN-γ, Neuro2A cells were co-cultured with recombinant murine IFN-γ (PeproTech Inc, Rocky Hill, USA; 50-30000 pg/ml) for 6, 12, 24 or 48 hours. After incubation, Neuro2A cells were either harvested to add Trypan blue and count the number of dead cells using a Bürker chamber, or ^3H-thymidine (MP Biomedicals, Irvine, CA; 1μCi/test) was added to count ^3H-thymidine uptake after incubation using a Microbeta TriLux counter (PerkinElmer, Shelton, USA).

Suppressor assay

To determine the ability of MDSC to inhibit T cell proliferation, splenic $CD3^-Gr1^+$MDSC were purified from RLI chimeras at day 35 using MACS, and were subsequently added in a 1:1 ratio to MACS-purified $CD3^+$ T cells from spleens of RLI chimeras at day 35 (responders) mixed with mitomycin C (Kyowa Hakko, Tokyo, Japan)-inactivated C57Bl/6 splenocytes (stimulators) or medium as control. On day 4 of incubation, ^3H-thymidine was added and cells were harvested after 18h of culture. ^3H-thymidine uptake was measured using a Microbeta TriLux counter.

FACS

FACS was performed using a LSR Fortessa (BD, Mountain View, CA, USA). PBL was collected by retro-orbital puncture and red blood cells were lysed using NH_4Cl. Spleen and LN were isolated and single cell suspensions were prepared. Tumors were excised, incubated in a mixture of Collagenase D (2mg/ml) and DNase (20μg/ml) (Sigma-Aldrich, Overijse, Belgium) in RPMI1640 containing 10% FCS, and leukocytes were separated by Percoll density gradient. Cells were stained with fluorochrome-conjugated mAb against CD45 (V500), CD3 (PerCP-Cy5.5), $H2K^b$ (FITC), CD4 (eF450), CD8 (APCeF780), CD19 (APCeF780), NK1.1 (APCeF780), CD11c (PerCPCy5.5), CD11b (eF450), Ly6C (PerCPCy5.5), Ly6G (APCeF780), IE^k (PE), IA^k (PE) (eBioscience, Vienna, Austria), $H2K^k$ (PE), CD80 (BV605) CD86 (BV510) (BD) and NKp46 (APC) (Biolegend, San Diego, USA). For intracellular stainings, cells were restimulated for 4 hours with 100 ng/ml PMA, 1 μg/ml ionomycin and 0.7 μg/ml monensin (Sigma-Aldrich) prior to surface staining. Cells were fixed, permeabilized and intracellularly stained with PE-conjugated anti-IFN-γ, anti-granzyme B or anti-Fas ligand (FasL) mAb (eBioscience). Intracellular FOXp3 was detected using the eBioscience Fixation & Permeabilization buffer set and allophycocyanin (APC)-conjugated anti-FOXp3 mAb (eBioscience). Data were analyzed with FlowJo software (Tree Star, Ashland, OR).

Cytometric bead array (CBA) assay

Release of TNF-α, IFN-γ, IL-2, IL-6, IL-10, IL-12 and IL-17 was quantified by a CBA assay (BD) according to the manufacturer's instructions. Samples were acquired using the LSR Fortessa and data were analyzed with FCAP Array software v3.0 (BD).

Statistical analysis

Statistical significance between 2 groups was determined by Mann-Whitney U test. Two-way ANOVA was performed to determine statistical significance between 2 groups on different time points. Log-rank test was used to determine statistical significance of survival curves. A P-value <0.05 was considered statistical significant. Statistics were performed using GraphPad Prism 6 Software.

Results

RLI alloreactivity is associated with a systemic cytokine storm and host T cell expansion.

As shown previously, infusion of recipient leukocytes (RLI) into mixed chimeras significantly delayed local neuroblastoma tumor growth (Fig. 1a) [12]. The anti-tumor effect coincided with strong host-anti-donor lymphohematopoietic alloreactivity as evident from a full rejection of donor T-, B-and NK-cell chimerism within 2 weeks after RLI (Fig. 1b). RLI-derived T cells but not NK cells were the mediators of alloreactivity: rejection still occurred when NK cell-depleted RLI was given, but donor chimerism remained unchanged after T cell-depleted RLI (Supplementary Figure 1).

Lymphohematopoietic alloreactivity was associated with a marked expansion of host $CD4^+$ T cells at day 35, and host $CD8^+$ T cells at day 28 and 35 post-alloBMT, compared to control chimeras. Donor $CD4^+$ and $CD8^+$ T cells were almost absent in RLI chimeras, consistent with the allorejection post-RLI. In control chimeras, low numbers of donor T cells on day 28 increased towards day 35, likely due to further donor engraftment post-alloBMT (Fig. 1c and d). B-and NK cell numbers were very low after RLI, since almost all B- and NK cells were donor-type at day 20 (Fig. 1b) and RLI fully rejects the donor B-and NK cell chimerism (Fig. 1e and f). As shown in Fig. 1g, the alloreactive response was also associated with an inflammatory cytokine storm: significantly elevated levels of IFN-γ, TNF-α, IL-6 and IL-10 were observed in serum of RLI chimeras as compared to control chimeras and naive animals, with levels peaking at day 26 post-alloBMT. Whereas IL-6 and IL-10 levels were only transiently enhanced, serum levels of IFN-γ and TNF-α remained significantly elevated. Serum levels of IL-2, IL-12 and IL-17 were not increased after RLI (Supplementary Figure 2).

RLI generates host CTL responses in spleen and LN.

To study the effector T cell pathways of the anti-tumor effect, flow cytometry was performed on spleens from chimeras at day 28 and 35 post-alloBMT. Absolute numbers of host-derived IFN-γ^+CD4^+ T lymphocytes were significantly higher in RLI chimeras compared to controls, both at day 28 and 35 (Fig. 2a). A trend towards increased numbers of host granzyme B^+CD4^+ T cells was also observed in RLI chimeras at day 28 that became significant by day 35 (Fig. 2b). The numbers of host IFN-γ^+CD8^+ T cells and granzyme B^+CD8^+ T cells were significantly higher in RLI chimeras than in controls at day 28 and 35 (Fig. 2c and d). Significantly enhanced numbers of host $FasL^+CD8^+$ T cells were also observed in RLI chimeras at day 35 compared to controls (Fig. 2e). A similar profile with increased expression of IFN-γ, granzyme B and FasL was observed in host $CD4^+$ and $CD8^+$ T lymphocytes in the LN of RLI chimeras (Supplementary Figure 3). Donor-type T helper 1 (Th1) cells and CTL were not detectable in spleens of RLI chimeras, due to full rejection of donor chimerism.

Consistent with the observation of a primed Th1 and CTL response, we observed an expansion in the frequency of $CD11c^+$ cells in the LN after RLI, together with a significant up-regulation in expression of CD80, CD86 and host MHC class II (MHC-II) (Fig. 3a-d).

Also consistent with the CTL expansion, $CD8^+$ T lymphocytes purified from spleens of RLI chimeras at day 28 or 35 showed significantly higher *ex vivo* cytotoxicity against Neuro2A than purified $CD8^+$ T cells from control chimeras and naive A/J mice (Fig. 2f and g). $CD8^+$ T cells from RLI chimeras also showed significantly higher killing activity against P815 than $CD8^+$ T cells from controls (Fig. 2h).

In conclusion, the RLI-induced lymphohematopoietic alloreactive response provides host CTL with killing activity against host-type neuroblastoma and a third-party tumor.

Neuroblastoma up-regulate MHC class I after RLI.

Cytokines may directly influence tumor immunogenicity by modulating expression of MHC class I (MHC-I) molecules. $H2K^k$ expression was significantly higher on tumor cells of RLI chimeras than on those of control chimeras, both at day 28 and 35 post-alloBMT (Fig. 4a). As demonstrated in Fig. 4b, *in vitro* co-culture of Neuro2A cells with IFN-γ or TNF-α for 48 hours showed that IFN-γ but not TNF-α significantly up-regulated $H2K^k$ on neuro2A cells, and this in a dose-dependent manner (Supplementary Figure 4). *In vitro* cultures of Neuro2A cells with increasing concentrations of IFN-γ resulted neither in increased numbers of dead Neuro2A cells, nor in decreased tumor proliferation (Supplementary Figure 5).

We conclude that Neuro2A cells up-regulate MHC-I in response to the cytokine storm. This is presumed to be –at least in part– mediated by IFN-γ while it has no direct killing effect against neuroblastoma.

RLI facilitates infiltration of host CTL into the tumor.

The tumor growth-inhibiting effect of RLI would require effector cells to infiltrate into the solid tumor environment. Effector T cell-numbers were analyzed within tumors from chimeras at day 28 and 35 post-alloBMT. Significantly higher numbers of host IFN-γ^+CD4^+ T cells were observed in tumors from RLI chimeras at day 28 compared to control chimeras. At day 35, the numbers had declined but were still significantly higher compared to controls. In tumors of both RLI and control chimeras, only low numbers of donor-type IFN-γ^+ $CD4^+$ T cells were present (Fig. 4c). Although host granzyme B^+CD4^+ T cells were shown to expand in spleens of RLI chimeras (Fig. 2b), this was not seen within the tumor (Fig. 4d). Significantly higher numbers of host IFN-γ^+CD8^+ T cells and granzyme B^+CD8^+ T cells were observed within tumors of RLI chimeras compared to controls, both at day 28 and 35, although the difference became smaller with time (Fig. 4e-f). The presence of IFN-γ-producing $CD8^+$ T cells was also confirmed by immunofluorescence stainings (Fig. 4g). In tumors of both RLI and control chimeras, donor-type IFN-γ^+CD8^+ and granzyme B^+CD8^+ T cells were very low, indicating that donor T cells contribute little to no anti-tumor reactivity (Fig. 4e and f). In conclusion,

the lymphohematopoietic response of RLI allows host Th1 cells and CTL to migrate into the solid tumor environment by day 28, but this effect seems transient as the absolute numbers have already strongly declined by day 35.

RLI-mediated alloreactivity induces an expansion of granulocytic and monocytic MDSC.

In contrast to the persisting effector T cell presence in the systemic compartment, within the tumor effector T cells seemed to decline by day 35. These opposing dynamics along with the observation that the tumor growth-inhibitory effect of RLI is incomplete, suggested that an immunoregulatory mechanism interferes with the intra-tumor effector pathway. We examined possible involvement of MDSC and T regulatory (Treg) cells, both of which have been reported as regulators of alloreactivity and anti-tumor reactivity [17–20]. MDSC can be induced by tumors as an immune escape mechanism [21], and are also known to be influenced in various contexts of immune stimulation and inflammation, such as auto-immunity, transplantation and alloreactivity [19,20,22]. We determined absolute numbers of the two major subsets: monocytic MDSC (M-MDSC; $CD11b^{+}Ly6G^{-}Ly6C^{+}$) and granulocytic MDSC (G-MDSC; $CD11b^{+}Ly6G^{+}Ly6C^{-}$), which have both shown to be immunosuppressive [22]. Whereas on day 28 clear differences in numbers of splenic MDSC could not be seen, on day 35 a strong expansion of host M-MDSC and G-MDSC was observed in RLI chimeras relative to controls (Fig. 5a and b). These expanded MDSC were able to functionally suppress T cell proliferation in RLI chimeras, as evident from *ex vivo* suppression assays showing significant inhibition of T cell proliferation when MDSC were added (Supplementary Figure 6). Donor M-MDSC or G-MDSC were not detected in spleens of RLI chimeras, consistent with the rejection of donor myeloid cells post-RLI (Fig. 5a and b). In the tumors of RLI chimeras, a small but significant increase in numbers of host M-MDSC and G-MDSC was observed by day 35. Donor-type MDSC were detected in low numbers due to the allorejection, while in control chimeras such donor M-MDSC and G-MDSC were clearly present (Fig. 5c and d).

No higher quantities of host and donor Treg cells were observed in RLI chimeras than in controls, both in spleen and tumor (Fig. 5e and f).

Together, the RLI-induced alloreactivity is followed by a strong splenic expansion of host-type M-MDSC and G-MDSC with potent T cell proliferation suppressive activity, which –although to a lesser extent– also become visible in the tumor environment.

MDSC depletion improves the anti-tumor effect of RLI.

We postulated that the MDSC accumulation is responsible for limiting the migration (and/or further expansion) of effector T cells into the tumor, hence also the incomplete RLI-effect in limiting tumor growth and improving survival (Fig. 1a). MDSC were depleted *in vivo* in RLI chimeras by injecting 5-FU (50mg/kg) on

day 30 post-alloBMT (Fig. 6a). 5-FU is a chemotherapeutic agent that was shown to selectively deplete MDSC within 5 days when administered at a low-dose (50mg/kg) [23]. FACS on spleens from RLI chimeras at day 35 showed that both M-MDSC and G-MDSC were indeed depleted after 5-FU treatment (Supplementary Figure 7). Strikingly, although RLI treatment in chimeras could not improve the overall survival relative to control chimeras, treatment of RLI chimeras with 5-FU resulted in significantly stronger tumor growth reduction and significantly prolonged survival, compared to chimeras treated with RLI only (Fig. 6b and c). Importantly, 5-FU was not able to impair local tumor growth in Neuro2A-bearing nonobese diabetic/severe combined immunodeficiency (NOD/SCID) mice (Supplementary Figure 8), indicating that 5-FU has no direct tumor killing effect. In conclusion, depletion of MDSC enhances the tumor growth-inhibitory effect of RLI at the local level as well as survival, suggesting that the MDSC expansion is –at least in part– responsible for the incomplete biological effect of RLI.

Discussion

In this study, we demonstrate that the lymphohematopoietic alloreactivity of RLI generates a host-derived cytotoxic T cell anti-neuroblastoma response, but also drives an expansion of host-type MDSC that counteracts the tumor growth-inhibitory effect of RLI. The MDSC expansion coincides with the decline of intra-tumor host-type effector T cells, presumably due to inhibition of migration of the systemically-generated effector cells into the tumor. Within the tumor MDSC also start to accumulate –albeit with a small delay– where they may directly inhibit T cell effector functions. These findings identify MDSC as a new target to improve the effectiveness of RLI, and possibly other cancer immunotherapies.

Expansion of host $CD4^+$ and $CD8^+$ T cells along with a cytokine storm and DC activation is observed in association with the RLI-induced alloreactivity. Analogous to the immune mechanisms proposed in RLI leukemia models [11,24], we postulate that the systemic alloresponse in tumor-bearing chimeras provides host T lymphocytes with cytotoxic potential against the solid neuroblastoma tumor. This is also evident from *ex vivo* $CD8^+$ T cell cytotoxicity assays, in which T cells derived from RLI chimeras showed enhanced killing activity against Neuro2A and a third-party tumor cell line. The latter observation indicates that the killing activity of CTL is –at least in part– non-specific.

Importantly, the systemic alloresponse and associated cytokine storm with DC activation seem to facilitate migration of the systemically-generated host effector T lymphocytes into the tumor, as evident from the intra-tumor accumulation of host-type Th1 cells and CTL. The finding of CTL within the tumor is in line with prior observations in murine leukemia models that pointed to IFN-γ-producing $CD8^+$ T cells and $CD4^+$ T-cell help in the anti-leukemia effector response of RLI [8]. RLI carries the additional advantage of rendering the tumor more susceptible to the effector CTL, as neuroblastoma cells up-regulated MHC-I after RLI. In line with reports on human tumor cells [25], Neuro2A up-regulated MHC-I in *in vitro* IFN-γ stimulation assays, based on which we presume that the up-regulation of MHC-I on Neuro2A tumor cells *in vivo* is –at least in part– mediated by IFN-γ. IFN-γ is released systemically during the cytokine storm, which most likely induces the MHC-I up-regulation on the tumor cells; IFN-γ is also produced within the tumor microenvironment by RLI-induced effector T cells, which presumably regulates the prolonged MHC-I up-regulation. This is in accordance with other studies reporting an important role for IFN-γ in the tumor microenvironment in allowing tumor responsiveness through various mechanisms, such as regulating CTL trafficking and up-regulating MHC-I [26,27].

Whereas previous work in the neuroblastoma model showed the presence of cytotoxic NK cells within tumors of RLI chimeras [12], our more recent data revealed that absolute numbers of such NK cells are very low as a consequence of full rejection of donor NK cell chimerism and slow NK cell recovery from the host compartment. Although this indicates that -relative to $CD8^+$ T cells- the role of NK cells in the baseline RLI-effect is probably limited, our prior observation that adoptive host NK cell therapy in RLI chimeras

enhanced the anti-tumor effect [12] indicates that the potential of NK cells may be synergistic and may be exploited in combination adoptive cell therapy.

The opposing dynamics of a persisting systemic and a declining intra-tumor effector T cell population along with a progressive systemic expansion of MDSC, led us hypothesize that the accumulating MDSC play a causal role in the incomplete RLI-effect on tumor growth and survival. Indeed, MDSC depletion in RLI chimeras using 5-FU resulted in significantly stronger inhibition of local tumor growth as well as improved overall survival. Although widely used as chemotherapeutic agent for several cancers including breast and colorectal cancer [28], low-dose 5-FU was shown in murine models to selectively trigger apoptosis in MDSC; *in vitro* and *in vivo* assays showed that administration of such low dose depletes MDSC without killing tumor cells or altering levels of other immune cells [23]. Analogously, low-dose 5-FU in RLI chimeras resulted in elimination of MDSC and in NOD/SCID mice we established that 5-FU had no direct Neuro2A killing effect.

MDSC accumulation occurs in a variety of conditions, first and foremost as immune-escape mechanism associated with tumor development [21,29]. Increased levels of MDSC-like cells have been detected in blood of neuroblastoma patients [30], however, in our neuroblastoma-bearing control chimeras this was not seen. MDSC expansion has also been documented in conditions of inflammation and auto-immunity in mouse models [22], and in association with alloHSCT and alloreactivity in mice and humans [20,31,32]. Because the MDSC expansion was seen exclusively in RLI chimeras and closely followed the donor chimerism rejection, we postulate that MDSC expand as a result of reactive host myelopoiesis -as observed in previous BMT models [18,19]- and the alloreactive inflammation. Specifically, given the known ability of IL-6 and IL1-β to drive MDSC accumulation [33], and IFN-γ to enhance the suppressor activity of MDSC [34–36], we postulate that the RLI-associated cytokine storm plays a critical role in driving MDSC expansion.

Since the intra-tumor CTL accumulation and splenic MDSC expansion show opposite and sequential dynamics, we hypothesize that the MDSC limit the migration of systemically-generated CTL into the tumor. MDSC release reactive nitrogen species such as peroxynitrite that can modify chemokines involved in CTL recruitment. For example, it was reported in murine models that peroxynitrite induces nitration of chemokine (C-C motif) ligand 2 (CCL2), thereby blocking T cell infiltration into the tumor [22,37]. MDSC possess, in addition to their inhibiting effect on lymphocyte trafficking, various other immune-inhibitory mechanisms [38–41], such as stimulation of tumor angiogenesis, stimulation of metastasis, negative modulation of the tumor microenvironment by inducing expansion of Treg cells and skewing of macrophage differentiation towards a pro-tumoral M2 phenotype. These mechanisms are potentially also involved in limiting the RLI-effect, and this is the subject of ongoing investigations. In addition to the strong MDSC expansion in the spleen, a quantitatively small but significant expansion of M-MDSC and to a lesser extent G-MDSC is seen in the tumor towards day 35 post-alloBMT. This delay -relative to the systemic

expansion- suggests that splenic MDSC also migrate into the tumor where they may directly inhibit CTL function. Of note, in contrast to the complete elimination of donor hematopoietic cells within 2 weeks following RLI, donor G-MDSC persist in tumors of RLI chimeras at day 28 and –to a lesser extent– at day 35. We postulate that the RLI-mediated allorejection of this donor-type cell population is more difficult within the tumor tissue than in the hematopoietic compartment, especially since RLI concurrently seems to drive an expansion of MDSC within this time frame.

MDSC can inhibit T cell functions via diverse mechanisms, including production of immunosuppressive cytokines (such as IL-10 and TGF-β), up-regulation of arginase 1 that depletes L-arginine and L-cysteine which are essential for T cell proliferation and cytotoxic activity, and production of reactive oxygen species and NO causing T cell hyporesponsiveness [21,42]. Although we have not investigated later time points, this effect may be progressive beyond day 35, when the tumor seems to escape the immune control and grows exponentially.

An expansion of cytotoxic $CD4^+$ T cells was also observed in the systemic compartment but within the tumor the results were inconsistent between animals. The existence of cytotoxic $CD4^+$ T cells has been increasingly recognized. In contrast to the well-known T helper function, recent findings indicate that $CD4^+$ T cells can exert cytotoxic functions when CTL are insufficient [43]. Homma *et al.* showed in a murine hepatocellular carcinoma model that the anti-tumor activity of a DC vaccine therapy was abrogated when $CD4^+$ T cells were depleted [44]. In a murine retrovirus-induced tumor model Akhmetzyanova *et al.* showed that tumor development coincided with granzyme B^+CD4^+ T cell expansion that induced complete tumor regression in the absence of Treg cells and $CD8^+$ T cells [45]. Since in our model granzyme B^+CD4^+ T cells were clearly induced in tumors of some RLI chimeras but not in others, we hypothesize that MDSC may also variably influence the influx and involvement of cytotoxic $CD4^+$ T cells in the RLI-effect.

Whereas RLI offers the critical advantage over DLI of not causing GvHD, its anti-tumor effect in leukemia and neuroblastoma models is significantly weaker than that of DLI [11,12,24]. MDSC have been shown in other transplant models to influence the critical balance between GvT and GvHD [19], and strikingly our current data indicate that by interfering with MDSC the anti-tumor effect of RLI can be enhanced while GvHD is still prevented. Of note, attempts with combination therapy using RLI and checkpoint inhibitor anti-PD-1 –given at a dose of 100 μg every 4 days– failed to augment the anti-tumor effects (unpublished observations). We speculate that this may be due to suppressive interference by the accumulating MDSC. Similarly, the MDSC may be responsible for the effect of adoptive NK cell therapy in previous studies, which was found to enhance the tumor growth-inhibitory effect of RLI but without improving overall survival [12].

Cancer immunotherapy is a rapidly evolving field, however, although durable responses have been obtained, for the majority of patients clinically relevant responses remain an elusive goal [46–48]. Several strategies under investigation use combined approaches triggering an effector response arm while

interfering with inhibitory pathways, giving promising results in both preclinical and clinical setting. Inhibition of IDO or $Gr1^{+}$myeloid cells increased T cell-mediated tumor-inhibitory effects of anti-CTLA-4 in murine models of melanoma and mammary carcinoma, respectively [49,50]. Moreover, Treg cell-depletion in renal cell carcinoma patients was shown to improve T cell responses mediated by DC vaccines [51]. In accordance with the observation in advanced renal cell carcinoma patients showing improved immune responses when MDSC were reduced [52], and a recent report showing that MDSC inhibition improved the efficacy of CAR therapy in sarcoma-bearing mice [53], our current data identify the MDSC regulatory pathway as a key intervention target for combination immunotherapy with RLI to improve its efficacy, not only for neuroblastoma but probably also for leukemia. Given the highly variable triggers of MDSC expansion and their diverse suppressor mechanisms, the MDSC pathway could be important in other types of cancer and anti-cancer immunotherapies.

Author contributions

Isabelle Dierckx de Casterlé designed and performed the experiments; acquired, analyzed and interpreted the data, and wrote the manuscript. Omer Rutgeerts and Caroline Lenaerts provided technical support in performing the experiments, and revised the manuscript. Sabine Fevery acquired flow cytometric data, participated in the interpretation of the data and revised the manuscript. Fariba Poosti and Sofie Struyf provided help in immunofluorescence stainings on tumor tissue. Mark Waer, An Billiau and Ben Sprangers conceived and supervised the study, contributed to the design of the experiments and interpretation of the data, and reviewed and edited the manuscript. All authors read and approved the final manuscript.

Acknowledgements

The authors gratefully acknowledge the Olivia Hendrickx Research Fund (www.olivia.be) and the Fund for Scientific Research (FWO) Flanders (www.FWO.be) for supporting this work with research grants, and the Olivia Hendrickx Research Fund for supporting Isabelle Dierckx de Casterlé with a fellowship grant. The authors thank Stefaan W. Van Gool for scientific advice on the tumor model, and Louis Boon for providing the anti-PD-1 (clone RMP1-14) mAb.

Funding

This work was supported by the Olivia Hendrickx Research Fund (www.olivia.be) and by the FWO grants G054010N (of A.D. Billiau) and 12V9218N (of F. Poosti).

Compliance with ethical standards

(1) Conflict of interest

The authors declare that they have no conflict of interest.

(2) Ethical approval and ethical standards

All procedures performed in the studies involving animals were ethically approved by the KU Leuven Animal Ethics Committee (Project approval number: P256/2014), and were in accordance with the ethical standards and guidelines of the KU Leuven. Animal care was in accordance with the KU Leuven guidelines for laboratory animals. All animals were obtained from external specialized companies (Envigo and Janvier Labs).

Figure legends

Fig. 1 Evolution of local tumor growth and alloreactivity after recipient leukocyte infusion

a. $1x10^6$ Neuro2A cells were inoculated s.c. in allogeneic chimeras on day 14 post-alloBMT, and chimeras received either recipient leukocyte infusion (RLI) on day 21 post-alloBMT ('alloBMT+RLI' ■) or no adoptive cell therapy ('alloBMT' ●). After tumors were established (usually around day 9 after tumor inoculation, i.e. day 23 post-alloBMT), tumor growth was measured twice weekly using a caliper and the volume (mm^3) was calculated ($width^2$ x length x 0.52). Results shown are from 2 identically designed experiments. **b.** Evolution of peripheral blood donor chimerism levels in total B cells (blue lines), NK cells (black lines) and T cells (green lines) in control chimeras ('alloBMT' ●, full lines) and chimeras treated with RLI on day 21 post-alloBMT ('alloBMT+RLI' ■, dotted lines). Results shown are from 4 experiments. **c-f.** Absolute numbers of $CD4^+$ T cells **(c)**, $CD8^+$ T cells **(d)** ('alloBMT' n=8-10; 'alloBMT+RLI' n=10-13), $CD19^+$ cells **(e)** ('alloBMT' n=6-9; 'alloBMT+RLI' n=6-10), and $NKp46^+$ cells **(f)** ('alloBMT' n=5-7; 'alloBMT+RLI' n=7-8) within host and donor compartment of spleens of RLI compared to control chimeras at day 28 and 35 post-alloBMT. **g.** Evolution of TNF-α, IFN-γ, IL-6 and IL-10 levels in serum from RLI chimeras ('alloBMT+RLI' ■, n=4-16), compared to control chimeras ('alloBMT' ●, n=3-12) and naive A/J mice (n=4). Bars represent SEM. *p<0.05, **p<0.01, ***p<0.001, ****p<0.0001.

Fig. 2 Induction of T helper 1 cells and CTL in the spleen after recipient leukocyte infusion

a-e. Absolute numbers of IFN-γ^+CD4^+ T cells **(a)**, granzyme B^+CD4^+ T cells **(b)**, IFN-γ^+CD8^+ T cells **(c)**, granzyme B^+CD8^+ T cells **(d)** ('alloBMT' n=9-13; 'alloBMT+RLI' n=12-15), and $FasL^+CD8^+$ T cells **(e)** ('alloBMT' n=6-9; 'alloBMT+RLI' n=6-11) within host and donor compartment of spleens of RLI compared to control chimeras at day 28 and 35 post-alloBMT. **f-h.** $CD8^+$ T cell reactivity against Neuro2A and P815 *ex vivo***.** Standard ^{51}Cr-release assays were performed to test cytotoxic activity of MACS-purified $CD8^+$ T cells derived from spleens of RLI chimeras ('alloBMT+RLI'), control chimeras ('alloBMT') or naive A/J mice against Neuro2A or P815. **f-g.** *Ex vivo* cytotoxicity against Neuro2A of $CD8^+$ T cells isolated from spleens of chimeras at day 28 post-alloBMT **(f)** or at day 35 post-alloBMT **(g)**. **h.** Cytotoxic capacity against P815 of $CD8^+$ T cells isolated from spleens of chimeras at day 35 post-alloBMT. Results shown represent specific lysis of tumor target cells at a 50:1 E:T ratio. Results shown are from 1-3 identically designed experiments. Bars represent SEM. *p<0.05, **p<0.01, ***p<0.001, ****p<0.0001.

Fig. 3 Expansion and activation of DC in the LN of RLI chimeras

LN were isolated from RLI and control chimeras at day 28 post-alloBMT. **a.** Frequency of $CD11c^+$ cells in RLI chimeras ('alloBMT+RLI' ■) compared to controls ('alloBMT' ●). **b-d.** MFI values (left) and representative

histograms (right) of the expression of CD80 **(b)**, CD86 **(c)** and IE^k and IA^k **(d)** on $CD11c^+$ cells in RLI chimeras ('alloBMT+RLI' ■, filled histogram) and control animals ('alloBMT' ●, open histogram). Results shown are from 3 identically designed experiments. Bars represent SEM. *p<0.05, **p<0.01, ****p<0.0001.

Fig. 4 MHC class I expression is enhanced on Neuro2A cells by IFN-γ, and higher numbers of host Th1 and CTL are found within tumors of RLI chimeras

a. Expression of $H2K^k$ on Neuro2A tumor cells *in vivo*, collected from RLI chimeras ('alloBMT+RLI' ■, n=5-6) and control animals ('alloBMT' ●, n=4-5) at day 28 and 35 post-alloBMT, determined by FACS. **b**. Expression of $H2K^k$ on Neuro2A cells, measured by FACS 48 hours after *in vitro* treatment of Neuro2A cells with medium (●, n=4), 500 pg/ml IFN-γ (◆, n=5), 100 pg/ml TNF-α (▲, n=5), or 500 pg/ml IFN-γ plus 100 pg/ml TNF-α (▼, n=5), i.e. similar concentrations as the *in vivo* serum levels found after RLI treatment. **c-f.** Tumor tissues of RLI chimeras ('alloBMT+RLI') and controls ('alloBMT') were collected at day 28 and 35 post-alloBMT to examine T cell infiltration into the tumor and cytotoxic profiles of intra-tumor T cells. Absolute numbers of IFN-γ^+CD4^+ T cells ('alloBMT' n=8-14; 'alloBMT+RLI' n=10-16) **(c)**, granzyme B^+CD4^+ T cells ('alloBMT' n=8-10; 'alloBMT+RLI' n=9-11) **(d)**, IFN-γ^+CD8^+ T cells ('alloBMT' n=8-14; 'alloBMT+RLI' n=10-16) **(e)**, and granzyme B^+CD8^+ T cells ('alloBMT' n=8-10; 'alloBMT+RLI' n=9-11) **(f)** at day 28 and 35 post-alloBMT within host and donor compartment of the tumor, normalized to 100 mm^3 tumor volume. Bars represent SEM. *p<0.05, **p<0.01, ****p<0.0001. **g.** IFN-γ (red) and CD8 (green) immunofluorescence stainings on tumor tissue sections of RLI chimeras ('alloBMT+RLI') and control chimeras ('alloBMT') at day 28 (upper panel) and 35 (lower panel) post-alloBMT. Scale bar, 50 μm.

Fig. 5 Expansion of host MDSC but not Treg cells in spleen and tumor of RLI chimeras

a-b. Absolute numbers of monocytic MDSC (M-MDSC; $CD11b^+Ly6G^-Ly6C^+$) **(a)** and granulocytic MDSC (G-MDSC; $CD11b^+Ly6G^+Ly6C^-$) **(b)** within host and donor compartment of <u>spleens</u> of RLI ('alloBMT+RLI' n=11-17) and control chimeras ('alloBMT' n=12-16) at day 28 and 35 post-alloBMT. **c-d.** Absolute numbers of M-MDSC **(c)** and G-MDSC **(d)** within host and donor compartment of <u>tumors</u> of RLI ('alloBMT+RLI' n=10-11) and control chimeras ('alloBMT' n=7-10) at day 28 and 35, normalized to 100 mm^3 tumor volume. **e.** Absolute numbers of regulatory T (Treg) cells ($CD4^+FOXp3^+$ cells) in host and donor compartment of <u>spleens</u> of RLI ('alloBMT+RLI' n=6-16) and control chimeras ('alloBMT' n=5-16), at day 28 and 35 post-alloBMT. **f.** Absolute numbers of Treg cells in host and donor compartment of <u>tumors</u> of RLI chimeras ('alloBMT+RLI' n=10-11) compared to controls ('alloBMT' n=9-10) at day 28 and 35, normalized to 100 mm^3 tumor volume. Bars represent SEM. *p<0.05, **p<0.01, ***p<0.001, ****p<0.0001.

Fig. 6 Biological effects of recipient leukocyte infusion combined with 5-FU to deplete MDSC

a. Recipient A/J mice received 9 Gy TBI followed by $5x10^6$ TCD alloBMC at day 0, and were inoculated s.c. with $1x10^6$ Neuro2A cells on day 14 post-alloBMT. Allogeneic chimeras received $50x10^6$ A/J splenocytes (RLI) on day 21 post-alloBMT and were injected i.p. with 50 mg/kg 5-FU or saline on day 30 post-alloBMT. **b-c.** Evolution of tumor volume **(b)** and survival **(c)** of Neuro2A-bearing allogeneic bone marrow chimeras given no adoptive cell therapy ('alloBMT' ●), or RLI with either 50 mg/kg 5-FU ('alloBMT+RLI+5-FU' ▲) or saline ('alloBMT+RLI' ■). Results shown are from 2 identically designed experiments. Bars represent SEM. *p<0.05, **p<0.01, ***p<0.001, ****p<0.0001. *Gy: Gray; TBI: Total body irradiation; TCD: T cell-depleted; alloBMC: allogeneic bone marrow cells.*

Supplementary Fig. 1 Alloreactivity after NK cell- or T cell-depleted recipient leukocyte infusion

Evolution of peripheral blood donor T cell chimerism at selected time points after transplantation, in chimeras treated with RLI ('alloBMT+RLI' ■, black dotted line), RLI from which NK cells were removed by MACS ('alloBMT+RLI w/o NK cells' ♦, blue line), T cell-depleted RLI ('alloBMT+RLI w/o T cells' ×, red line) or no RLI ('alloBMT' ●, black full line). Bars represent SEM. *p<0.05, **p<0.01, ***p<0.001, ****p<0.0001.

Supplementary Fig. 2 Recipient leukocyte infusion is not associated with production of IL-2, IL-12 or IL-17

Evolution of IL-2, IL-12 and IL-17 levels in serum from RLI chimeras ('alloBMT+RLI' ■, n=4-17), compared with control chimeras ('alloBMT' ●, n=3-12) and naive A/J mice (n=4). Bars represent SEM.

Supplementary Fig. 3 Recipient leukocyte infusion increases expression of cytotoxic markers on host T cells in the LN

a-e. Cytotoxic profile of host $CD4^+$ and $CD8^+$ T cells in the LN of RLI ('alloBMT+RLI') and control chimeras ('alloBMT'), at day 28 and 35 post-alloBMT. IFN-γ expression on host $CD4^+$ T cells ('alloBMT' n=9-10; 'alloBMT+RLI' n=11-12) **(a)**, granzyme B production by host $CD4^+$ T cells ('alloBMT' n=11-16; 'alloBMT+RLI' n=12-19) **(b)**, IFN-γ on host $CD8^+$ T cells ('alloBMT' n=10-12; 'alloBMT+RLI' n=13-16) **(c)**, granzyme B expression on host $CD8^+$ T lymphocytes ('alloBMT' n=11-16; 'alloBMT+RLI' n=12-19) **(d)** and FasL expression on host $CD8^+$ T lymphocytes ('alloBMT' n=6-9; 'alloBMT+RLI' n=6-11) **(e)**. Bars represent SEM. *p<0.05, **p<0.01, ****p<0.0001.

Supplementary Fig. 4 IFN-γ treatment enhances $H2K^k$ expression on Neuro2A cells *in vitro* in a dose-dependent manner

Neuro2A cells were co-cultured *in vitro* for 48 hours with increasing concentrations of IFN-γ (0-300000

pg/ml), followed by flow cytometric analysis to determine the expression of $H2K^k$ on Neuro2A cells (MFI values are shown). Result shown is from 1 experiment. Bars represent SEM.

Supplementary Fig. 5 IFN-γ has no direct killing effect on Neuro2A cells *in vitro*

a. Neuro2A cells were co-cultured with different concentrations of IFN-γ (0-300000 pg/ml) for 6, 12, 24 or 48 hours, and cell viability was assessed by a Trypan blue exclusion assay. Result shown is from 1 experiment (n=4 per time point). **b.** Tumor cell proliferation was measured 24 and 48 hours after treatment of Neuro2A cells with increasing concentrations of IFN-γ (0-300000 pg/ml). Result shown is from 1 experiment (n=4 per time point). Bars represent SEM.

Supplementary Fig. 6 RLI-induced MDSC suppress T cell proliferation *ex vivo*

MACS-purified $CD3^+$ T cells from day 35 spleens of RLI chimeras (n=4) were stimulated with mitomycin C-inactivated C57Bl/6 splenocytes ('C57Bl/6') or medium (control for proliferation). MACS-purified $CD3^-Gr1^+$ MDSC from day 35 spleens of the same RLI chimeras were added in a 1:1 MDSC:T cell ratio. Day 4 after culture, ^{3}H-thymidine was added and T cell proliferation was assessed after 18h by measuring ^{3}H-thymidine incorporation. Results shown are from 1 experiment. Bars represent SEM. *$p<0.05$.

Figures

Fig. 1

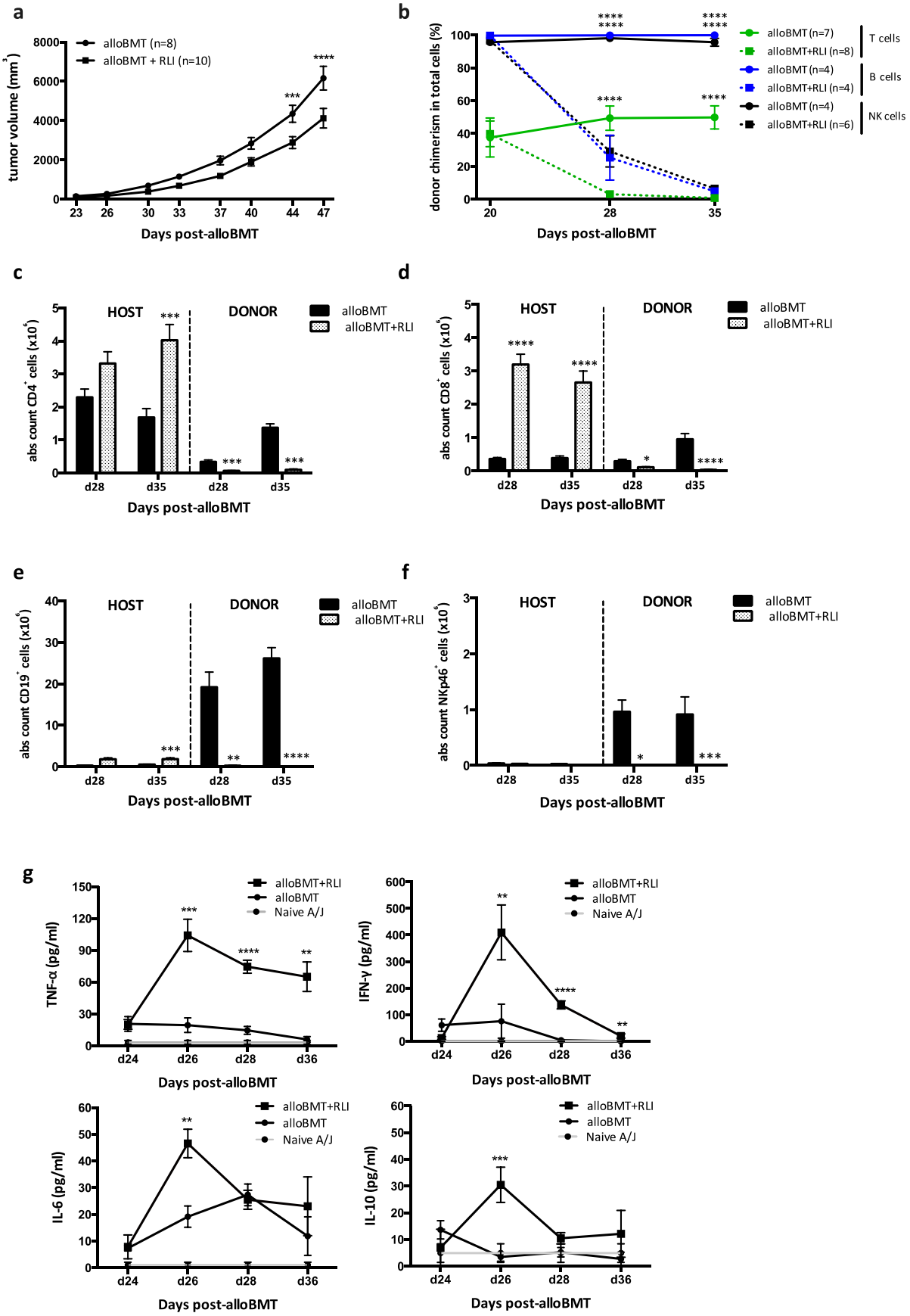

Fig. 2

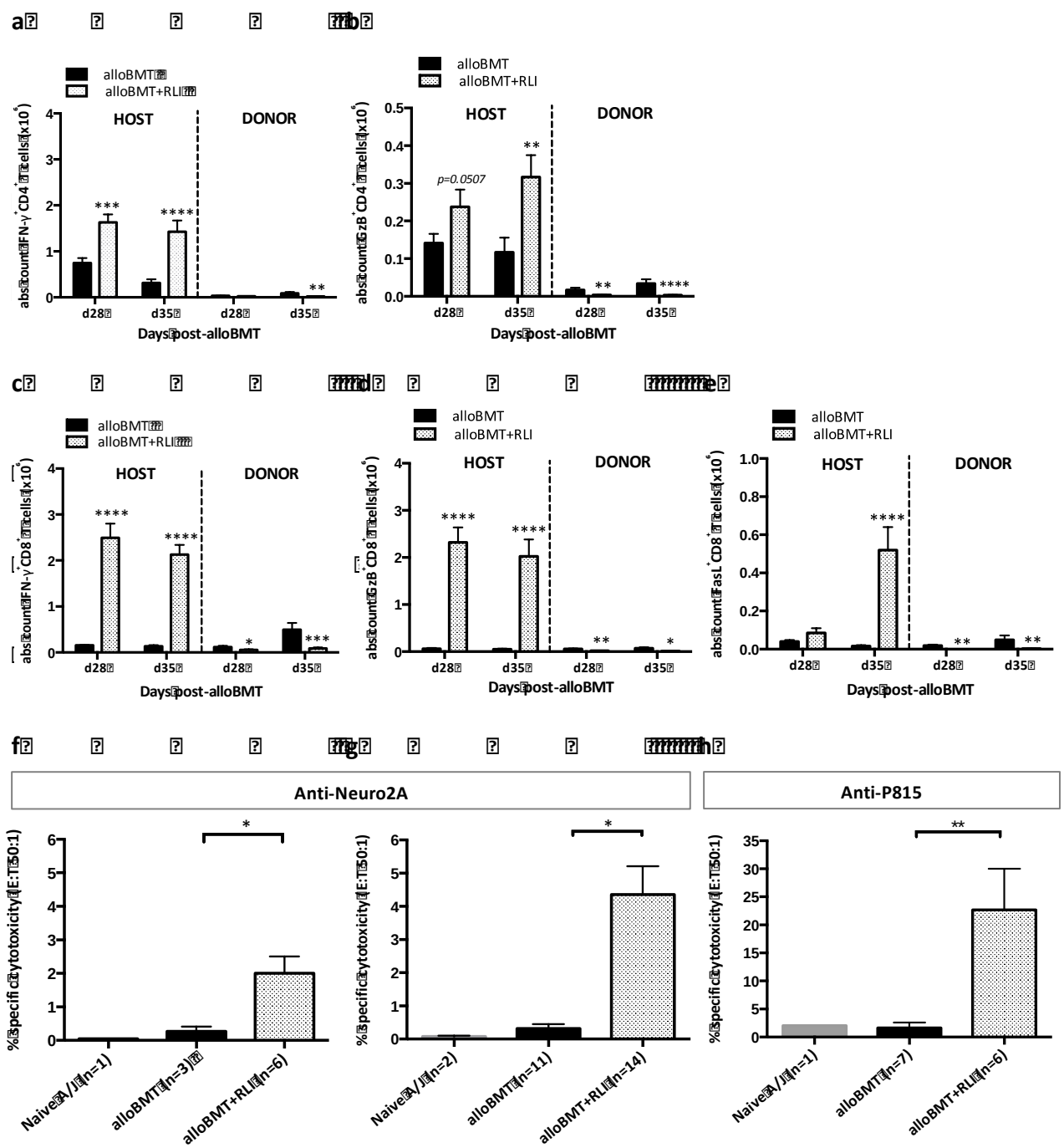
a
b
c
d
e
f
g
h
alloBMT
alloBMT+RLI
HOST
DONOR
d28
d35
Days post-alloBMT
p=0.0507
Anti-Neuro2A
Anti-P815
Naive (n=1)
alloBMT (n=3)
alloBMT+RLI (n=6)
Naive (n=2)
alloBMT (n=11)
alloBMT+RLI (n=14)
Naive (n=1)
alloBMT (n=7)
alloBMT+RLI (n=6)

Fig. 3

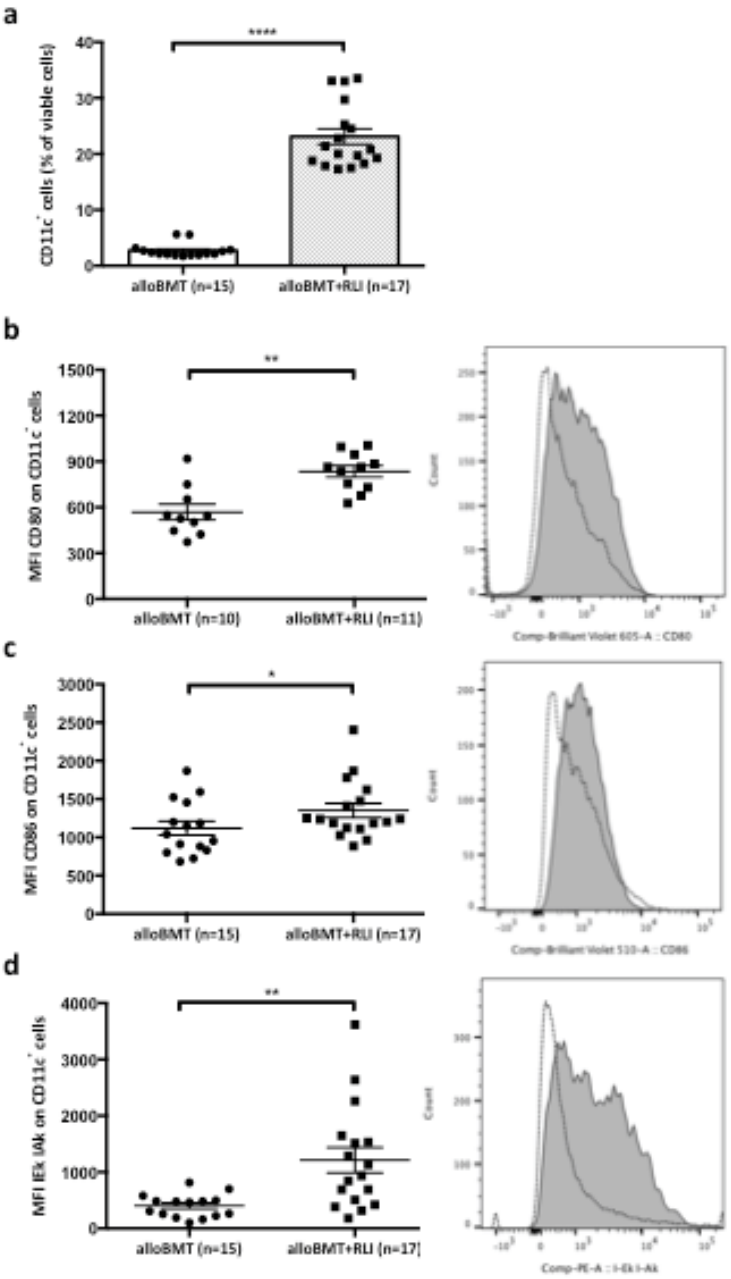
a
****
CD11c+ cells (% of viable cells)
40
30
20
10
0
alloBMT (n=15)
alloBMT+RLI (n=17)
b
**
MFI CD80 on CD11c+ cells
1500
1200
900
600
300
0
alloBMT (n=10)
alloBMT+RLI (n=11)
Count
Comp-Brilliant Violet 605-A :: CD80
c
*
MFI CD86 on CD11c+ cells
3000
2500
2000
1500
1000
500
0
alloBMT (n=15)
alloBMT+RLI (n=17)
Count
Comp-Brilliant Violet 510-A :: CD86
d
**
MFI IEk IAk on CD11c+ cells
4000
3000
2000
1000
0
alloBMT (n=15)
alloBMT+RLI (n=17)
Count
Comp-PE-A :: I-Ek I-Ak

Fig. 4

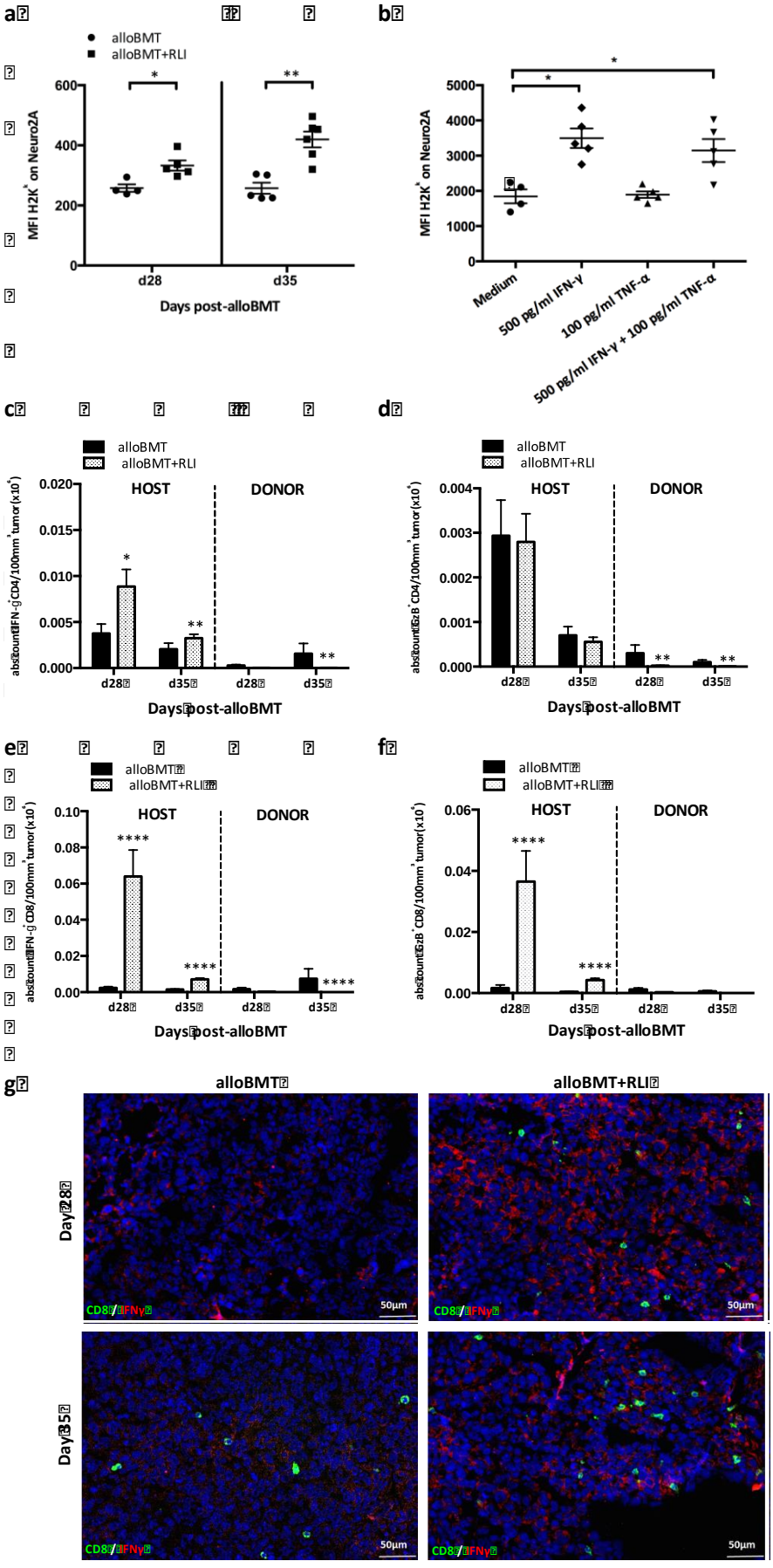
a
alloBMT
alloBMT+RLI
MFI H2K* on Neuro2A
d28
d35
Days post-alloBMT
b
MFI H2K* on Neuro2A
Medium
500 pg/ml IFN-γ
100 pg/ml TNF-α
500 pg/ml IFN-γ + 100 pg/ml TNF-α
c
alloBMT
alloBMT+RLI
HOST
DONOR
Days post-alloBMT
d
alloBMT
alloBMT+RLI
HOST
DONOR
Days post-alloBMT
e
alloBMT
alloBMT+RLI
HOST
DONOR
Days post-alloBMT
f
alloBMT
alloBMT+RLI
HOST
DONOR
Days post-alloBMT
g
alloBMT
alloBMT+RLI
Day 28
Day 35
CD8/IFNγ
50μm

Fig. 5

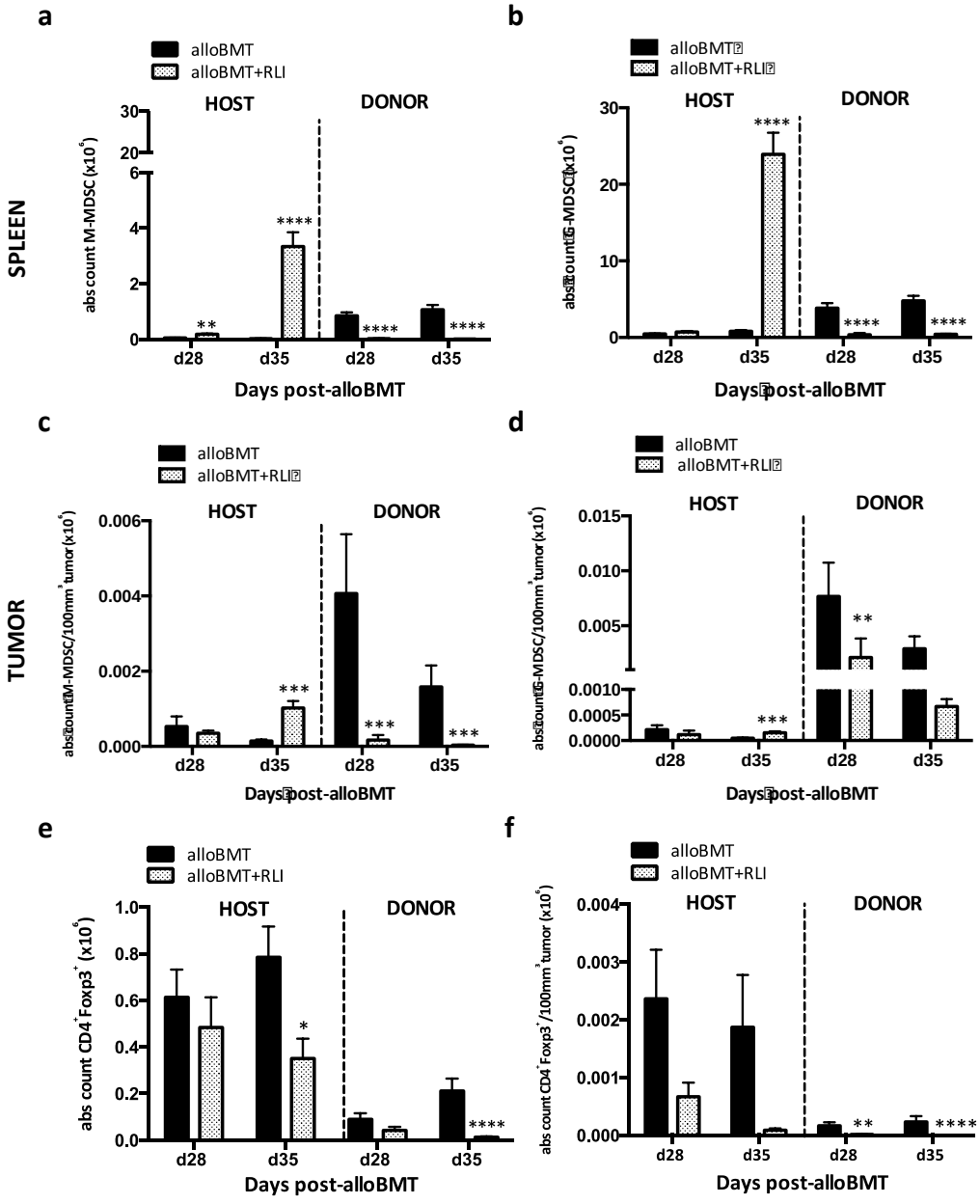
a
b
c
d
e
f
SPLEEN
TUMOR
alloBMT
alloBMT+RLI
HOST
DONOR
d28
d35
Days post-alloBMT
abs count M-MDSC (x10^6)
abs count G-MDSC (x10^6)
abs count M-MDSC/100mm^3 tumor (x10^6)
abs count G-MDSC/100mm^3 tumor (x10^6)
abs count CD4+Foxp3+ (x10^6)
abs count CD4+Foxp3+/100mm^3 tumor (x10^6)

Fig. 6

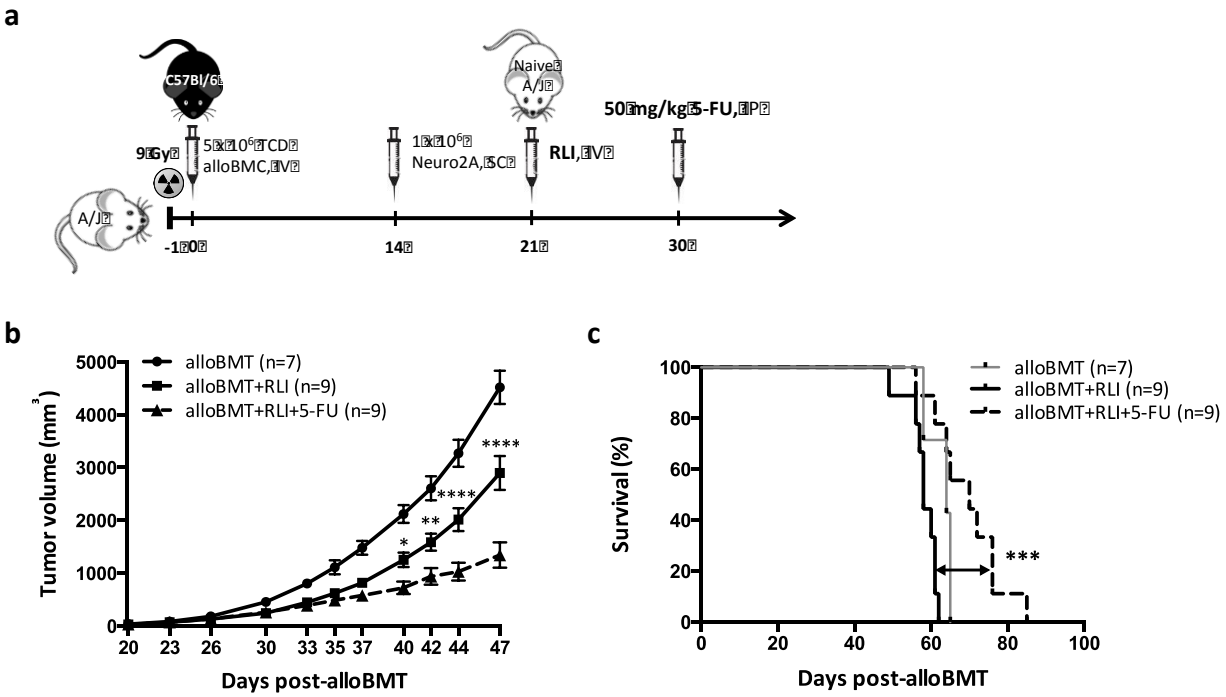
a
C57Bl/6
Naive
A/J
9 Gy
5 x 10^6 TCD
alloBMC, IV
1 x 10^6
Neuro2A, SC
RLI, IV
50 mg/kg 5-FU, IP
A/J
-1
0
14
21
30
b
alloBMT (n=7)
alloBMT+RLI (n=9)
alloBMT+RLI+5-FU (n=9)
Tumor volume (mm3)
Days post-alloBMT
c
alloBMT (n=7)
alloBMT+RLI (n=9)
alloBMT+RLI+5-FU (n=9)
Survival (%)
Days post-alloBMT

Supplementary Fig. 1

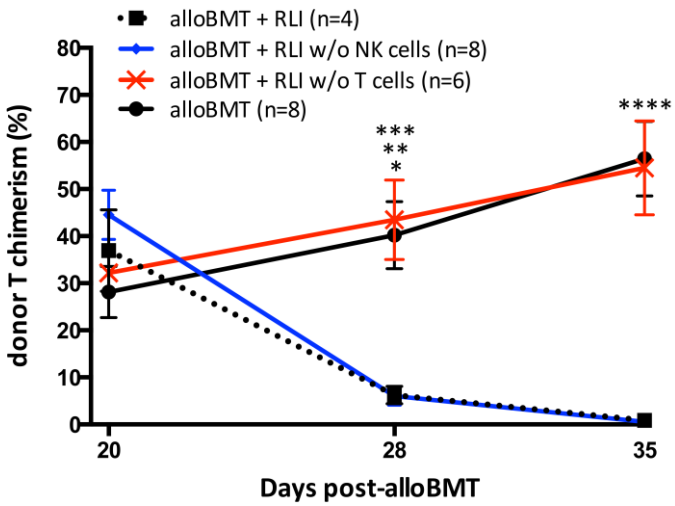

Supplementary Fig. 2

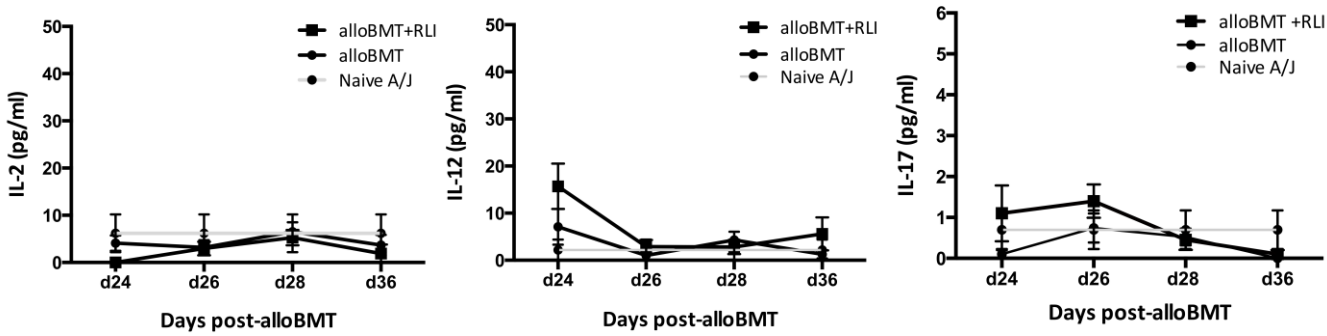

Supplementary Fig. 3

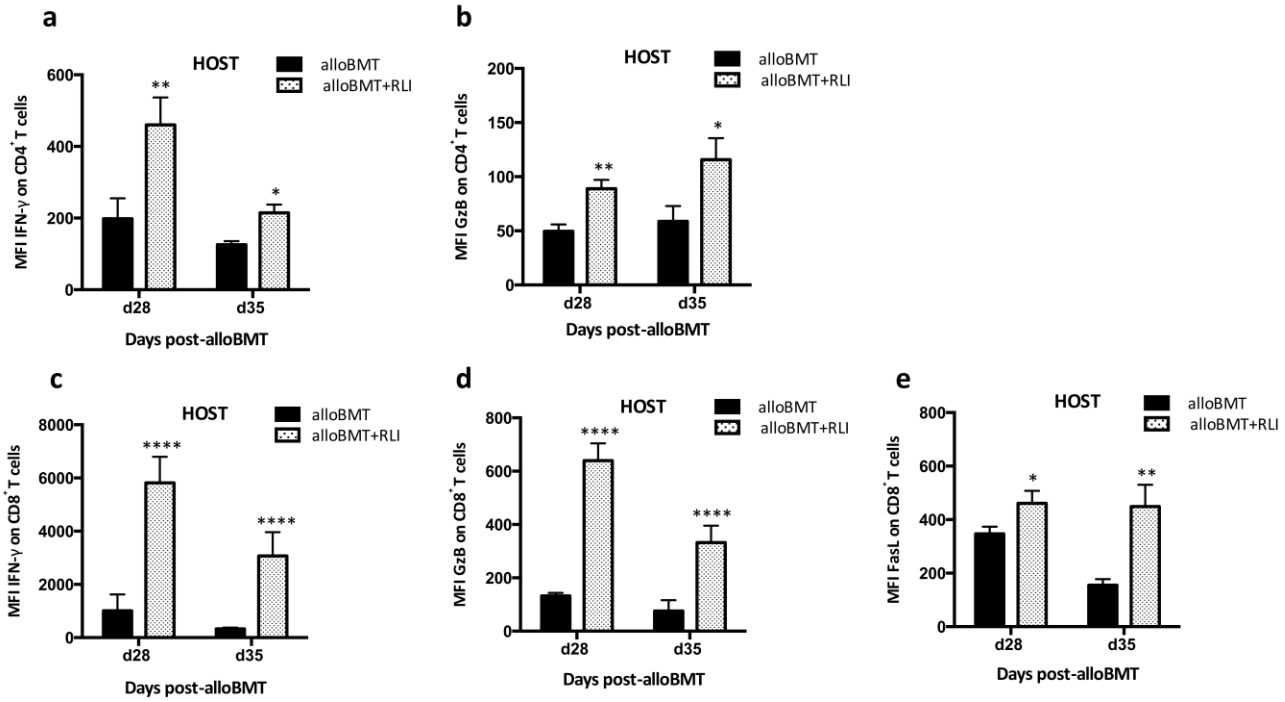

Supplementary Fig. 4

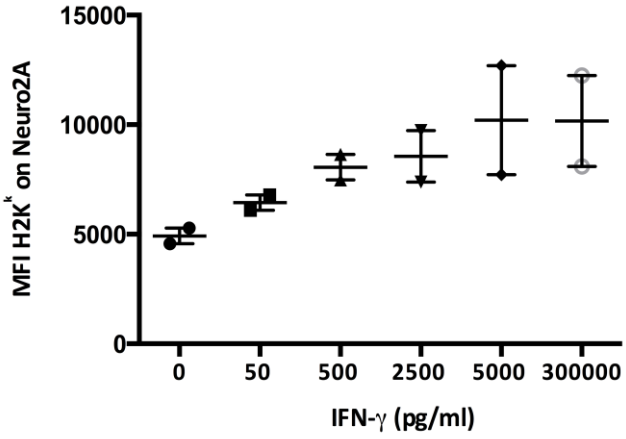

Supplementary Fig. 5

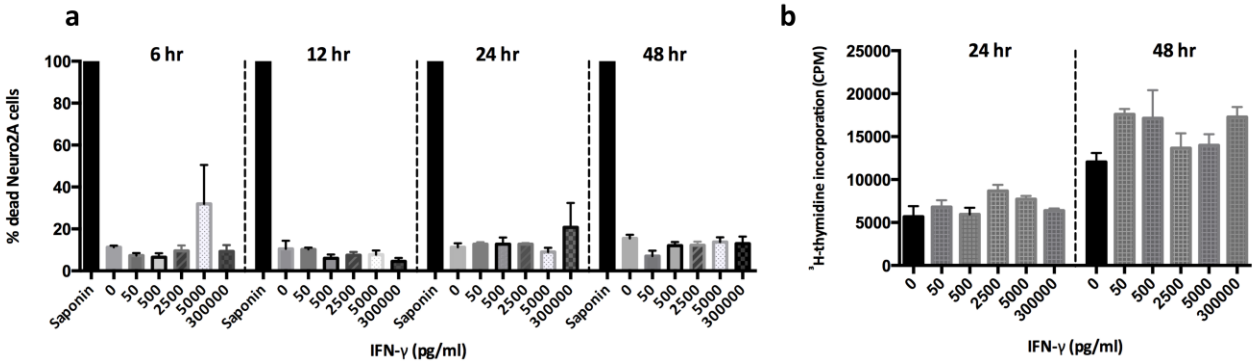

Supplementary Fig. 6

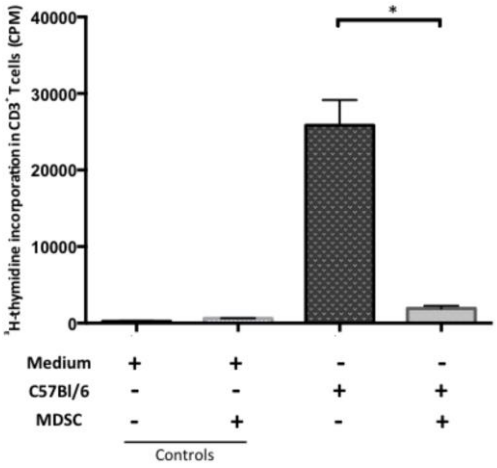

References

[1] Zahid MF, Ali N, Shaikh MU, Adil SN (2014) Outcome of allogeneic hematopoietic stem cell transplantation in patients with hematological malignancies. Int J Hematol Oncol Stem Cell Res 8:30–8.

[2] Demirer T, Barkholt L, Blaise D, Pedrazzoli P, Aglietta M, Carella AM, et al (2008) Transplantation of allogeneic hematopoietic stem cells: an emerging treatment modality for solid tumors. Nat Clin Pract Oncol 5:256–67.

[3] Kanold J, Paillard C, Tchirkov A, Merlin E, Marabelle A, Lutz P, et al (2008) Allogeneic or haploidentical HSCT for refractory or relapsed solid tumors in children: toward a neuroblastoma model. Bone Marrow Transplant 42 Suppl 2:S25-30.

[4] Hale GA, Arora M, Ahn KW, He W, Camitta B, Bishop MR, et al (2013) Allogeneic hematopoietic cell transplantation for neuroblastoma: the CIBMTR experience. Bone Marrow Transplant 48:1056–64.

[5] Ho VT, Soiffer RJ (2001) The history and future of T-cell depletion as graft-versus-host disease prophylaxis for allogeneic hematopoietic stem cell transplantation. Blood 98:3192–204.

[6] Rager A, Porter DL (2011) Cellular therapy following allogeneic stem-cell transplantation. Ther Adv Hematol 2:409–28.

[7] Dey BR, McAfee S, Colby C, Cieply K, Caron M, Saidman S, et al (2005) Anti-tumour response despite loss of donor chimaerism in patients treated with non-myeloablative conditioning and allogeneic stem cell transplantation. Br J Haematol 128:351–9.

[8] Rubio MT, Saito TI, Kattleman K, Zhao G, Buchli J, Sykes M (2005) Mechanisms of the antitumor responses and host-versus-graft reactions induced by recipient leukocyte infusions in mixed chimeras prepared with nonmyeloablative conditioning: a critical role for recipient CD4+ T cells and recipient leukocyte infusion-derived IFN-gamma-producing CD8+ T cells. J Immunol 175:665–76.

[9] Rubio MT, Zhao G, Buchli J, Chittenden M, Sykes M (2006) Role of indirect allo- and autoreactivity in anti-tumor responses induced by recipient leukocyte infusions (RLI) in mixed chimeras prepared with nonmyeloablative conditioning. Clin Immunol 120:33–44.

[10] Saito TI, Li HW, Sykes M (2010) Invariant NKT cells are required for antitumor responses induced by host-versus-graft responses. J Immunol 185:2099–105.

[11] De Somer L, Sprangers B, Fevery S, Rutgeerts O, Lenaerts C, Boon L, et al (2011) Recipient

lymphocyte infusion in MHC-matched bone marrow chimeras induces a limited lymphohematopoietic host-versus-graft reactivity but a significant antileukemic effect mediated by CD8+ T cells and natural killer cells. Haematologica 96:424–31.

[12] Willems L, Fevery S, Sprangers B, Rutgeerts O, Lenaerts C, Ibrahimi A, et al (2013) Recipient leukocyte infusion enhances the local and systemic graft-versus-neuroblastoma effect of allogeneic bone marrow transplantation in mice. Cancer Immunol Immunother 62:1733–44.

[13] Morgenstern DA, Baruchel S, Irwin MS (2013) Current and future strategies for relapsed neuroblastoma: challenges on the road to precision therapy. J Pediatr Hematol Oncol 35:337–47.

[14] Bartholomew J, Washington T, Bergeron S, Nielson D, Saggio J, Quirk L (2016) Dinutuximab: A Novel Immunotherapy in the Treatment of Pediatric Patients With High-Risk Neuroblastoma. J Pediatr Oncol Nurs 34:5-12.

[15] Siapati KE, Barker S, Kinnon C, Michalski A, Anderson R, Brickell P, et al (2003) Improved antitumour immunity in murine neuroblastoma using a combination of IL-2 and IL-12. Br J Cancer 88:1641–8.

[16] Sefrioui H, Billiau AD, Waer M (2000) Graft-versus-leukemia effect in minor antigen mismatched chimeras given delayed donor leucocyte infusion: immunoregulatory aspects and role of donor T and ASGM1-positive cells. Transplantation 70:348-53.

[17] De Somer L, Fevery S, Bullens DM, Rutgeerts O, Lenaerts C, Mathieu C, et al (2010) Murine bone marrow chimeras developing autoimmunity after CTLA-4-blockade show an expansion of T regulatory cells with an activated cytokine profile. Immunol Lett 133:49-53.

[18] Billiau AD, Fevery S, Rutgeerts O, Landuyt W, Waer M (2003) Transient expansion of Mac1+Ly6-G+Ly6-C+ early myeloid cells with suppressor activity in spleens of murine radiation marrow chimeras: possible implications for the graft-versus-host and graft-versus-leukemia reactivity of donor lymphocyte infusions. Blood 102:740-8.

[19] Sprangers B, Van Wijmeersch B, Luyckx A, Sagaert X, Verbinnen B, Rutgeerts O, et al (2011) Subclinical GvHD in non-irradiated F1 hybrids: severe lymphoid-tissue GvHD causing prolonged immune dysfunction. Bone Marrow Transplant 46:586–96.

[20] Luyckx A, Schouppe E, Rutgeerts O, Lenaerts C, Koks C, Fevery S, et al (2012) Subset characterization of myeloid-derived suppressor cells arising during induction of BM chimerism in mice. Bone Marrow Transplant 47:985–92.

[21] Umansky V, Blattner C, Gebhardt C, Utikal J (2016) The role of myeloid-derived suppressor cells (MDSC) in cancer progression. Vaccines (Basel) 4:36.

[22] Gabrilovich DI, Nagaraj S (2009) Myeloid-derived suppressor cells as regulators of the immune system. Nat Rev Immunol 9:162–74.

[23] Vincent J, Mignot G, Chalmin F, Ladoire S, Bruchard M, Chevriaux A, et al (2010) 5-Fluorouracil selectively kills tumor-associated myeloid-derived suppressor cells resulting In enhanced T cell-dependent antitumor immunity. Cancer Res 70:3052-61.

[24] Saito TI, Rubio MT, Sykes M (2006) Clinical relevance of recipient leukocyte infusion as antitumor therapy following nonmyeloablative allogeneic hematopoietic cell transplantation. Exp Hematol 34:1271–7.

[25] Prigione I, Corrias MV, Airoldi I, Raffaghello L, Morandi F, Bocca P, et al (2004) Immunogenicity of human neuroblastoma. Ann. N. Y. Acad. Sci. 1028:69–80.

[26] Alshaker HA, Matalka KZ (2011) IFN-γ, IL-17 and TGF-β involvement in shaping the tumor microenvironment: The significance of modulating such cytokines in treating malignant solid tumors. Cancer Cell Int 11:33.

[27] Lugade AA, Sorensen EW, Gerber SA, Moran JP, Frelinger JG, Lord EM (2008) Radiation-induced IFN-gamma production within the tumor microenvironment influences antitumor immunity. J Immunol 180:3132–9.

[28] Longley DB, Harkin DP & Johnston PG (2003) 5-Fluorouracil: mechanisms of action and clinical strategies. Nature Rev Cancer 3:330–8.

[29] Melero I, Rouzaut A, Motz GT, Coukos G (2014) T-cell and NK-cell infiltration into solid tumors: a key limiting factor for efficacious cancer immunotherapy. Cancer Discov 4:522-6.

[30] Santilli G, Piotrowska I, Cantilena S, Chayka O, D'Alicarnasso M, Morgenstern DA, et al (2013) Polyphenol E enhances the antitumor immune response in neuroblastoma by inactivating myeloid suppressor cells. Clin Cancer Res 19:1116–25.

[31] Wang D, Yu Y, Haarberg K, Fu J, Kaosaard K, Nagaraj S, et al (2013) Dynamic change and impact of myeloid-derived suppressor cells in allogeneic bone marrow transplantation in mice. Biol Blood Marrow Transplant 19:692–702.

[32] Yin J, Wang C, Huang M, Mao X, Zhou J, Zhang Y (2016) Circulating CD14(+) HLA-DR(-/low) myeloid-derived suppressor cells in leukemia patients with allogeneic hematopoietic stem cell transplantation: novel clinical potential strategies for the prevention and cellular therapy of graft-versus-host disease. Cancer Med 5:1654–69.

[33] Bunt SK, Yang L, Sinha P, Clements VK, Leips J, Ostrand-Rosenberg S (2007) Reduced inflammation in the tumor microenvironment delays the accumulation of myeloid-derived suppressor cells and limits tumor progression. Cancer Res 67:10019–26.

[34] Mazzoni A, Bronte V, Visintin A, Spitzer JH, Apolloni E, Serafini P, et al (2002) Myeloid suppressor lines inhibit T cell responses by an NO-dependent mechanism. J Immunol 168:689–95.

[35] Bronte V (2009) Myeloid-derived suppressor cells in inflammation: Uncovering cell subsets with enhanced immunosuppressive functions. Eur J Immunol 39:2670–2.

[36] Ostrand-Rosenberg S, Sinha P (2009) Myeloid-derived suppressor cells: linking inflammation and cancer. J Immunol 182:4499–506.

[37] Molon B, Ugel S, Del Pozzo F, Soldani C, Zilio S, Avella D, et al (2011) Chemokine nitration prevents intratumoral infiltration of antigen-specific T cells. J Exp Med 208:1949–62.

[38] Ugel S, De Sanctis F, Mandruzzato S, Bronte V (2015) Tumor-induced myeloid deviation: when myeloid-derived suppressor cells meet tumor-associated macrophages. J Clin Invest 125:3365–76.

[39] Motallebnezhad M, Jadidi-Niaragh F, Qamsari ES, Bagheri S, Gharibi T, Yousefi M (2016) The immunobiology of myeloid-derived suppressor cells in cancer. Tumor Biol 37:1387–406.

[40] Sinha P, Clements VK, Bunt SK, Albelda SM, Ostrand-Rosenberg S (2007) Cross-talk between myeloid-derived suppressor cells and macrophages subverts tumor immunity toward a type 2 response. J Immunol 179:977–83.

[41] Marvel D, Gabrilovich DI (2015) Myeloid-derived suppressor cells in the tumor microenvironment : expect the unexpected. J Clin Invest 125:3356–64.

[42] Kumar V, Patel S, Tcyganov E, Gabrilovich DI (2016) The nature of myeloid-derived suppressor cells in the tumor microenvironment. Trends Immunol 37:208–20.

[43] Haabeth OA, Tveita AA, Fauskanger M, Schjesvold F, Lorvik KB, Hofgaard PO, et al (2014) How do CD4+ T cells detect and eliminate tumor cells that either lack or express MHC class II molecules?

Front Immunol 5:174.

[44] Homma S, Komita H, Sagawa Y, Ohno T, Toda G (2005) Antitumour activity mediated by CD4+ cytotoxic T lymphocytes against MHC class II-negative mouse hepatocellular carcinoma induced by dendritic cell vaccine and interleukin-12. Immunology 115:451–61.

[45] Akhmetzyanova I, Zelinskyy G, Schimmer S, Brandau S, Altenhoff P, Sparwasser T, et al (2013) Tumor-specific CD4+ T cells develop cytotoxic activity and eliminate virus-induced tumor cells in the absence of regulatory T cells. Cancer Immunol Immunother 62:257–71.

[46] Stewart TJ, Smyth MJ (2011) Improving cancer immunotherapy by targeting tumor-induced immune suppression. Cancer Metastasis Rev 30:125–40.

[47] Gajewski TF (2015) The next hurdle in cancer immunotherapy: overcoming the non-T-cell-inflamed tumor Microenvironment. Semin Oncol 42:663–71.

[48] Farkona S, Diamandis EP, Blasutig IM (2016) Cancer immunotherapy: the beginning of the end of cancer? BMC Med 14:73.

[49] Holmgaard RB, Zamarin D, Munn DH, Wolchok JD, Allison JP (2013) Indoleamine 2,3-dioxygenase is a critical resistance mechanism in antitumor T cell immunotherapy targeting CTLA-4. J Exp Med 210:1389–402.

[50] Stewart TJ, Liewehr DJ, Steinberg SM, Greeneltch KM, Abrams SI (2009) Modulating the Expression of IFN Regulatory Factor 8 Alters the Protumorigenic Behavior of CD11b+Gr-1+ Myeloid Cells. J Immunol 183:117–28.

[51] Dannull J, Su Z, Rizzieri D, Yang BK, Coleman D, Yancey D, et al (2005) Enhancement of vaccine-mediated antitumor immunity in cancer patients after depletion of regulatory T cells. J Clin Invest 115:3623–33.

[52] Mirza N, Fishman M, Fricke I, Dunn M, Neuger AM, Frost TJ, et al (2006) All-trans-retinoic acid improves differentiation of myeloid cells and immune response in cancer patients. Cancer Res 66:9299–307.

[53] Long AH, Highfill SL, Cui Y, Smith JP, Walker AJ, Ramakrishna S, et al (2016) Reduction of MDSCs with All-trans Retinoic Acid Improves CAR Therapy Efficacy for Sarcomas. Cancer Immunol Res 4:869–80.